velocity in cartesian coordinates with accuracy greater than 0.1 mm and 1.3 mm s^{-1}, respectively.

Jerk was estimated by applying a fourth-order Savitsky–Golay filter on a 250-ms window of velocity data. This filter is equivalent to taking the second derivative at the window's centre of the continuous least-squares best-fit fourth-order polynomial. This fourth-order polynomial fit is a low-pass filter with a cutoff frequency of 6.83 Hz. Power spectra of mean subtracted velocity profiles of very fast 10-cm reaching movements show that 99.9% of the power is below 6 Hz.

We assessed motion state transition efficiency using cumulative squared jerk to characterize the efficiency of recovery after perturbation offset. To accomplish this, we compared the amount of jerk that occurred between two different motion states within the same movement, with the jerk that would occur for a maximally smooth transition between those two states in the elapsed time. The minimum jerk trajectory between two motion states (state = [position, velocity, acceleration]) is given by a fifth-order polynomial in time:

$$x(t) = C_5(t/t_f)^5 + C_4(t/t_f)^4 + C_3(t/t_f)^3 + C_2(t/t_f)^2 + C_1(t/t_f) + C_0$$

Where position is represented by $x(t)$, t is time and t_f is the final time. C_ks are parameters that depend on the boundary motion states and on the time between them, t_f. They can be found by solving the boundary conditions on the motion state.

Once the coefficients are determined the cumulative squared jerk can be computed by simply integrating the squared jerk profile.

$$j(t) = x(t) = [60C_5(t/t_f)^2 + 24C_4(t/t_f) + 6C_3]/t_f^3$$

$$\text{Cumulative Squared Jerk} = \int_0^{t_f} j^2(t)\mathrm{d}t$$

Received 26 August; accepted 3 November 1999.

1. Folstein, S. E. *Huntington's Disease a Disorder of Families* (Johns Hopkins Univ. Press, Baltimore, 1989).
2. The Huntington's Disease Collaborative Research Group. A novel gene containing a trinucleotide repeat that is expanded and unstable on Huntington's disease chromosomes. *Cell* **72,** 971–983 (1993).
3. Aylward, E. H. *et al.* Longitudinal change in basal ganglia volume in patients with Huntington's disease. *Neurology* **48,** 394–399 (1997).
4. Aylward, E. H. *et al.* Basal ganglia volume and proximity to onset in presymptomatic Huntington disease. *Arch Neurol.* **53,** 1293–1296 (1996).
5. Brandt, J. *et al.* Clinical correlates of dementia and disability in Huntington's disease. *J. Clin. Neuropsychol.* **6,** 401–412 (1984).
6. Shadmehr, R. & Mussa-Ivaldi, F. A. Adaptive representation of dynamics during learning of a motor task. *J. Neurosci.* **14,** 3208–3224 (1994).
7. Shidara, M., Kawano, K., Gomi, H. & Kawato, M. Inverse-dynamics model eye movement control by Purkinje cells in the cerebellum. *Nature* **365,** 50–52 (1993).
8. Bhushan, N. & Shadmehr, R. Computational nature of human adaptive control during learning of reaching movements in force fields. *Biol. Cybern.* **81,** 39–60 (1999).
9. Shadmehr, R. & Brashers-Krug, T. Functional stages in the formation of human long-term motor memory. *J. Neurosci.* **17,** 409–419 (1997).
10. Flash, T. & Hogan, N. The coordination of arm movements: an experimentally confirmed mathematical model. *J. Neurosci.* **5,** 1688–1703 (1985).
11. Miall, R. C., Weir, D. J. & Stein, J. F. Manual tracking of visual targets by trained monkeys. *Behav. Brain Res.* **20,** 185–201 (1986).
12. Wolpert, D. M., Ghahramani, Z. & Jordan, M. I. Are arm trajectories planned in kinematic or dynamic coordinates? An adaptation study. *Exp. Brain Res.* **103,** 460–470 (1995).
13. Cordo, P. J. Kinesthetic control of a multijoint movement sequence. *J. Neurophysiol.* **63,** 161–172 (1990).
14. Atkeson, C. G. & Hollerbach, J. M. Kinematic features of unrestrained vertical arm movements. *J. Neurosci.* **59,** 2318–2330 (1985).
15. Meyer, B. U. *et al.* Motor responses evoked by magnetic brain stimulation in Huntington's Disease. *Electroencephalogr. Clin. Neurophysiol.* **85,** 197–208 (1992).
16. Noth, J., Podoll, K. & Friedemann, H. H. Long-loop reflexes in small hand muscles studied in normal subjects and in patients with Huntington's Disease. *Brain* **108,** 65–80 (1985).
17. Kuwert, T. *et al.* Comparison of somatosensory evoked potentials with striatal glucose consumption measured by positron emission tomography in the early diagnosis of Huntington's Disease. *Mov. Disord.* **8,** 98–106 (1993).
18. Topper, R., Schwarz, M., Podoll, K., Domges, F. & Noth, J. Absence of frontal somatosensory evoked potentials in Huntington's Disease. *Brain* **116,** 87–101 (1993).
19. Foroud, T. *et al.* Cognitive scores in carriers of Huntington's disease gene compared to noncarriers. *Ann. Neurol.* **37,** 657–664 (1995).
20. de Boo, G. M. *et al.* Early cognitive and motor symptoms in identified carriers of the gene for Huntington disease. *Arch. Neurol.* **54,** 1353–1357 (1997).
21. Siemers, E. *et al.* Motor changes in presymptomatic Huntington disease gene carriers. *Arch. Neurol.* **53,** 487–492 (1996).
22. Rothlind, J. C., Brandt, J., Zee, D., Codori, A. M. & Folstein, S. Unimpaired verbal memory and oculomotor control in asymptomatic adults with the genetic marker for Huntington's disease. *Arch. Neurol.* **50,** 799–802 (1993).
23. Blackmore, L., Simpson, S. A. & Crawford, J. R. Cognitive performance in UK sample of presymptomatic people carrying the gene for Huntington's disease. *J. Med. Genet.* **32,** 358–362 (1995).
24. Kuwert, T. *et al.* Striatal glucose consumption in chorea-free subjects at risk of Huntington's disease. *J. Neurol.* **241,** 31–36 (1993).
25. Mazziotta, J. C. *et al.* Reduced cerebral glucose metabolism in asymptomatic subjects at risk for Huntington's Disease. *N. Engl. J. Med.* **316,** 357–362 (1987).
26. Gabrieli, J. D., Stebbins, G. T., Singh, J. Willingham, D. B. & Goetz, C. G. Intact mirror-tracing and impaired rotary-pursuit skill learning in patients with Huntington's Disease: Evidence for dissociable memory systems in skill learning. *Neuropsychology* **11,** 272–281 (1997).
27. Hogan, N. in *Multiple Muscle Systems* (eds Winters, J. M. & Woo, S. L. Y.) 149–164 (Springer, New York, 1990).
28. Miall, R. C. & Wolpert, D. M. Forward models for physiologic motor control. *Neur. Net.* **9,** 1265–1279 (1996).
29. Schultz, W., Dayan, P. & Montague, P. R. A neural substrate of prediction and reward. *Science* **275,** 1593–1599 (1997).

Acknowledgements

We thank K. Thoroughman and N. Bhushan. R.S. and M.S. conceived of the experiments, M.S. collected the data, and designed and carried out the data analysis guided by interaction with R.S., J.B., N.B. and K.T. M.S. and R.S. wrote the manuscript. The Johns Hopkins HD Center (director C. A. Ross) arranged patient visits and clinical assessment of HD patients. The work was supported by grants from the Whitaker Foundation (R.S.) and the National Institutes of Health (R.S. and J.B.), and a pre-doctoral fellowship from the National Institute of General Medical Sciences to M.S.

Correspondence and requests for materials should be addressed to M.S. (e-mail: msmith@bme.jhu.edu).

A neuronal analogue of state-dependent learning

D. E. Shulz*, R. Sosnik†, V. Ego*, S. Haidarliu† & E. Ahissar†

† *Department of Neurobiology, The Weizmann Institute of Science, 76100 Rehovot, Israel*

* *Equipe Cognisciences, UNIC, Institut A. Fessard, CNRS, 91198 Gif sur Yvette, France*

State-dependent learning is a phenomenon in which the retrieval of newly acquired information is possible only if the subject is in the same sensory context and physiological state as during the encoding phase[1]. In spite of extensive behavioural and pharmacological characterization[2], no cellular counterpart of this phenomenon has been reported. Here we describe a neuronal analogue of state-dependent learning in which cortical neurons show an acetylcholine-dependent expression of an acetylcholine-induced functional plasticity. This was demonstrated on neurons of rat somatosensory 'barrel' cortex, whose tunings to the temporal frequency of whisker deflections were modified by cellular conditioning. Pairing whisker stimulation with acetylcholine applied iontophoretically yielded selective lasting modification of responses, the expression of which depended on the presence of exogenous acetylcholine. Administration of acetylcholine during testing revealed frequency-specific changes in response that were not expressed when tested without acetylcholine or when the muscarinic antagonist, atropine, was applied concomitantly. Our results suggest that both acquisition and recall can be controlled by the cortical release of acetylcholine.

The ascending cholinergic system[3] has long been considered to be a candidate for mediating behavioural control of neuronal plasticity[4–9]. This hypothesis is supported by behavioural and neurophysiological studies in the auditory[10–13] and somatosensory systems[14–18]. Whereas these studies demonstrated the permissive role of acetylcholine (ACh) during the induction of cortical plasticity[10–14], they did not address the possibility that ACh is also involved in the expression of the induced modifications. To examine this potential role of ACh, single- ($n = 99$) and multi-unit ($n = 85$) activities were recorded extracellularly from the barrel field[19] of anaesthetized adult rats, using a multi-electrode array composed of one or two tungsten-in-glass electrodes and one combined electrode for recording and iontophoresis of ACh. Temporal-frequency tuning curves (TFTCs)

were obtained by mechanically deflecting the principal vibrissa at four different frequencies between 2 and 11 Hz (in a few cases 14 Hz was also applied), covering the frequency range predominantly used by the animal while exploring its environment[20]. Typically, TFTCs of barrel cortex neurons show decreased spike counts and increased latencies with increasing frequencies[21]. The TFTC was determined again during ACh iontophoresis, and then pairing occurred. Pairing consisted of repetitive whisker deflection at one fixed frequency (5, 8 or 11 Hz) accompanied by ACh iontophoresis. After pairing, the TFTC was determined, once without ACh and once during application of ACh, thereby restoring the physiological conditions under which the pairing was carried out.

Pairing caused frequency-specific modification of the TFTCs that was expressed exclusively under ACh application. Three examples of significant increments in response, induced by pairing and revealed with ACh, are depicted in Fig. 1 (Fig. 1a–c, two-tailed Kolmogorov–Smirnov, $P < 0.0005$ compared with control). The principal whisker for each cell was stimulated at 5 (Fig. 1a), 8 (Fig. 1b) or 11 Hz (Fig. 1c) during pairing. The potentiation of the response was maximal for the conditioned frequency in each case and affected both the phasic (due to each whisker deflection) and tonic (due to the entire train of deflections) components of the response. The summed response (phasic + tonic per stimulus cycle) is referred to herein as 'responsiveness'. No change was expressed when the responses were recorded without ACh (Fig. 1a–c, Kolmogorov–Smirnov test, $P > 0.1$). The modifications could be reversed by a second pairing using a different stimulation frequency. A new frequency-specific enhancement in response after a second pairing is shown in Fig. 1d. Usually, the second pairing resulted also in a significant reduction of response to the initially paired frequency (11 Hz, Fig. 1d) (see Supplementary Information). When the extinction of the effect was analysed by repeatedly testing the TFTC without and with ACh, the response modification was still statistically significant at least 45 min after the pairing but only under ACh (four out of four cells, two-tailed Kolmogorov–Smirnov, $P < 0.0005$). The consistent lack of expression without ACh, during periods that were interleaved with successful expression with ACh, excludes the possibility that the observed effects correspond to a delayed expression of cholinergic-induced plasticity[22] (see Supplementary Information).

Overall, 33% (39 out of 119) of the single- and multi-units recorded with the combined electrode showed a statistically significant TFTC modification when tested with ACh after pairing. In contrast, when measured without ACh, TFTC changes were observed in fewer cases (21%, 25 out of 119; χ^2 test, $P < 0.05$). This difference was also valid for single units: 30% showed a modified TFTC (17 out of 57) when tested with ACh, whereas only 14% (8 out of 57) were modified when measured without ACh (χ^2 test, $P < 0.05$). Most of the changes expressed with ACh were response potentiations specific to the paired frequency (76%). Consistent with studies in the auditory cortex[10], most of the effects observed during testing without ACh were decreases in responsive-

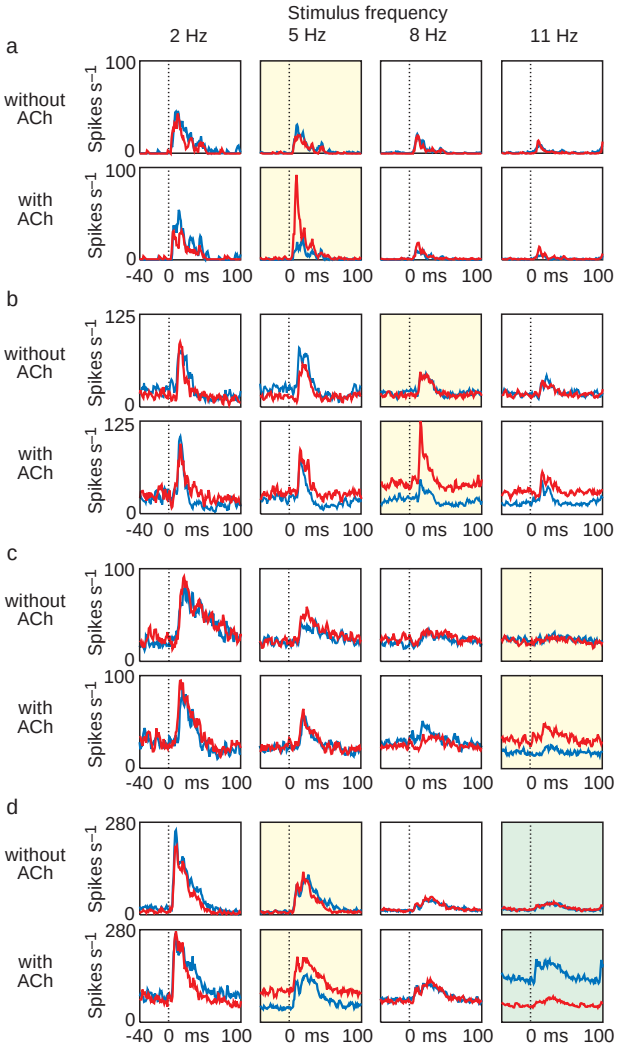

Figure 1 Plasticity of cortical responses expressed during ACh application in four different units. Peri-stimulus time histograms of responses before (blue) and after (red) pairing are superimposed. The activity preceding the stimulus onset (dashed lines) corresponds to the cell's tonic activation during the stimulus train. Yellow shading indicates the paired frequency. Pairing at 5 (**a**), 8 (**b**) and 11 Hz (**c**) resulted in an enhanced response to the paired frequency when tested with ACh (Kolmogorov–Smirnov, $P < 0.0005$), but not when tested without ACh ($P > 0.1$) (**a**–**c**). **d**, Reversal of the potentiation induced by a first conditioning at 11 Hz (green shading, $P < 0.0005$), by a second pairing at 5 Hz (yellow shading, $P < 0.0005$). No change was revealed when testing without ACh ($P > 0.9$).

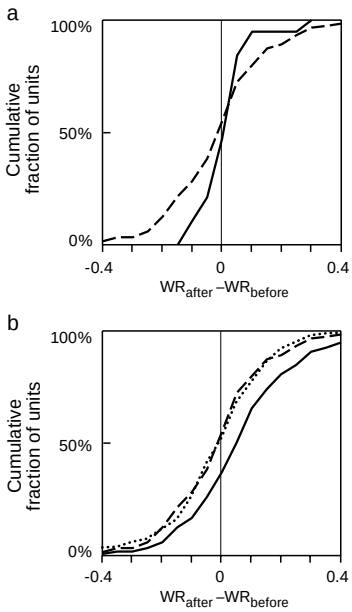

Figure 2 Statistical analysis of ACh-induced response modifications for all tested units. **a**, Cumulative distribution of response changes ($WR_{after} - WR_{before}$; see Methods for definition of weighted ratio (WR)) plotted for cells tested for temporal stability of TFTCs without ACh ($n = 19$, solid line) and with ACh ($n = 40$, dashed line). **b**, Cumulative distributions of changes between the second and fourth TFTCs. Changes in responses of the paired group ($n = 119$) to the paired (solid line) and the unpaired (dotted line) frequencies and in responses of the unpaired control group to all frequencies ($n = 40$, dashed line).

ness (87.5%). The overlap between the populations of cells displaying significant TFTC changes after pairing with and without ACh was small: only 3 out of the 22 modified single units showed effects in both conditions.

We tested whether ACh application is required during pairing in order to induce TFTC changes by repeating the pairing protocol without ACh. In most cases (17 out of 19), whisker stimulation without ACh induced no changes in the TFTC. Additional evidence supporting the permissive role of ACh in the induced plasticity was obtained from cells recorded simultaneously with a tungsten-in-glass electrode other than the combined electrode used for iontophoresis. Only 7% of the units (3 out of 45) recorded with tungsten-in-glass electrodes (that is, units that were probably beyond the maximal distance from the ejection site where ACh is still effective in modifying neuronal firing activity (S. H. *et al.*, unpublished data)) were modified after pairing when tested with ACh, even though they were activated by the stimulus. In contrast, 33% (39 out of 119) of the cells simultaneously recorded by the combined electrode were significantly modified (χ^2 test, $P < 0.002$), confirming that the modifications are observed preferentially within the region of ACh application.

Part of the response modifications described here may have resulted from the presence of ACh during the second and fourth TFTCs of the protocol and not from the pairing. To isolate the effect of the fixed-frequency pairing, the population of cells submitted to pairing was compared with a control population for which the four TFTCs were applied with no conditioning period in between (the time interval between the second and the third TFTCs was kept the same as for the original protocol). Responses were quantified by a weighted ratio between the response to stimulation at a given frequency and the averaged response to all other frequencies (see Methods). Figure 2 shows the cumulative distributions of changes in weighted ratio observed in each condition. Consistent with other studies[23,24], and independently of the pairing, the response variability was larger (two-tailed *F*-test, $P < 0.001$) when tested with ACh (Fig. 2a, dashed line) than without ACh (Fig. 2a, solid line), whereas the mean was unchanged (two-tailed Mann-Whitney *U*-test, $P > 0.46$). However, the introduction of the fixed-frequency pairing induced an additional effect: the relative strength of the response to the paired frequency was significantly potentiated (Fig. 2b, compare solid and dashed curves, one-tailed Mann–Whitney *U*-test, $P < 0.001$), whereas the variability was unchanged (two-tailed *F*-test, $P > 0.37$). These potentiations were specific for the paired frequency, as the distribution of changes for unpaired frequencies (Fig. 2b, dotted line) was indistinguishable from the control distribution (Fig. 2b, dashed line, two-tailed Mann–Whitney *U*-test, $P > 0.1$), and significantly different from the distribution of changes at the paired frequency (Fig. 2b, solid line, two-tailed Mann–Whitney *U*-test, $P < 0.0001$).

Statistically, the entire population was potentiated by fixed-frequency pairings. However, when each unit was analysed separately, only a subpopulation exhibited significant modifications. We examined the dependency of these modifications on the frequency of the paired stimulus (Fig. 3). The significant potentiations observed during testing with ACh were maximal for the paired frequency (Fig. 3a–c) and differed from changes at other frequencies (Fig. 3d–f; analysis of variance (ANOVA), $F(1,43) = 5.45$, 6.68 and 6.43 for 5, 8 and 11 Hz, respectively, $P < 0.05$). On average, the TFTCs' reorganization after pairing was such that paired and unpaired frequencies showed, respectively, relative gains and losses in response (Fig. 3g, right box; ANOVA, $F(1,43) = 12.07$, $P < 0.005$). No significant reorganization of the TFTCs was observed when testing without ACh (Fig. 3g, left box; ANOVA, $F(1,43) = 0.45$, $P > 0.5$).

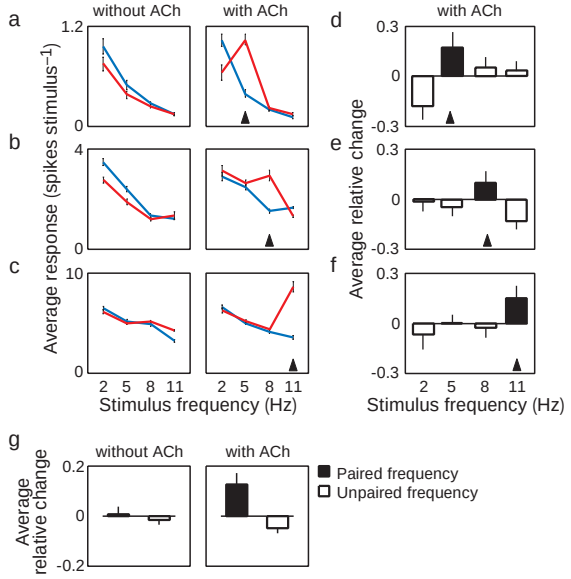

Figure 3 Reorganization of TFTCs expressed with ACh after pairing. **a–c**, Average responses (± s.e.m.) to different stimulation frequencies. Three examples showing significant (Kolmogorov–Smirnov, $P < 0.0005$) response enhancements to the paired frequency (5, 8 or 11 Hz) with ACh (blue before, red after pairing, arrowheads indicate the paired frequency). TFTCs tested without ACh were unchanged ($P > 0.4$) (**a,b**) or showed smaller changes ($P < 0.002$) (**c**). **d–f,** For all units significantly potentiated at any frequency when tested with ACh, the response changes for each frequency were averaged across units submitted to pairings at 5 (**d**), 8 (**e**) or 11 (**f**) Hz. Response changes to the paired (black bars) and non-paired (white bars) frequencies differ within each group (ANOVA; $P < 0.05$). **g**, Changes in responses to paired and non-paired frequencies averaged across all potentiated cells tested with and without ACh.

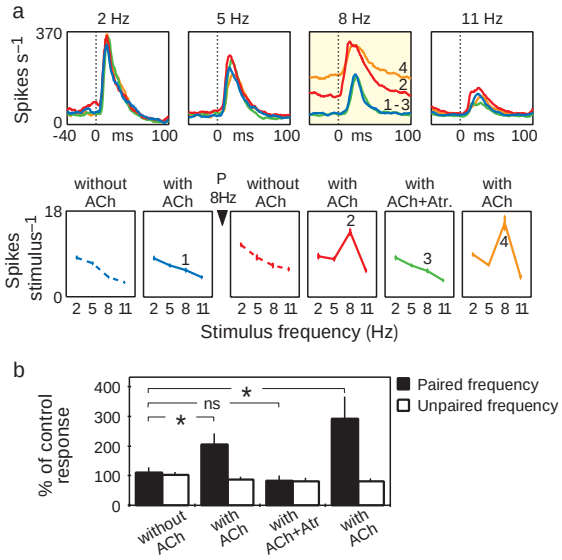

Figure 4 Atropine blocks the ACh-dependent expression of plasticity. **a**, Top row, peristimulus time histograms of responses before (blue), and after pairing tested with ACh (red), with ACh and atropine (green), and again with ACh (orange) are superimposed for each frequency. Bottom row, TFTCs (mean response ± s.e.m.) of the unit shown in the top row before (blue) and after (red, green, orange) pairing at 8 Hz (P). TFTCs obtained without ACh are shown as dashed lines. Numbers (1–4) indicate the response levels corresponding to the histograms numbered in the top row (8 Hz). **b**, Mean (± s.e.m.) percentage of change in response to stimulation at paired (black bars) and unpaired (white bars) frequencies compared with control (in chronological order: tested without ACh, with ACh, with ACh and atropine (Atr), and again with ACh). Asterisk, two-tailed Student's *t*-test, $P < 0.05$, $n = 5$; ns, not significant.

The ACh-dependent expression of the enhancement in response to the paired frequency was blocked by the muscarinic antagonist, atropine. Figure 4 shows an example of a significant frequency-specific potentiation (Fig. 4a, 8 Hz, red line; Kolmogorov–Smirnov, $P < 10^{-7}$) that is absent when atropine and ACh are iontophoresed together during testing (Fig. 4a, green line; Kolmogorov–Smirnov, $P > 0.89$). Two minutes after the end of atropine application, a significantly enhanced response to the paired frequency was recovered with ACh (Fig. 4a, orange line; Kolmogorov–Smirnov, $P < 10^{-7}$). Overall, the muscarinic nature of the effect has been confirmed in all the cells showing an ACh-dependent expression of plasticity and tested with atropine (five out of five cells; Fig. 4b).

The temporal response properties of populations of auditory cortical cells can be modified after extensive periods of tone presentations at a given repetition rate paired with stimulation of the nucleus basalis[13]. We have shown that single units of the somatosensory barrel cortex can show a rapidly induced ACh-dependent plasticity of temporal response properties. Furthermore, we have shown that the expression of ACh-induced modifications is also regulated by increased cortical ACh. The altered responsiveness to a specific stimulus frequency, which was associated with increased ACh levels, was expressed only in the presence of ACh. The requisite for a similarity between the acquisition and the recall conditions is analogous to a "state-dependent learning"[1,2]—a phenomenon in which newly acquired information may become available for retrieval only if the endogenous state of the brain and the sensory context present at the time of the original encoding episode are reinstated at the time of testing. In our anaesthetized animals, the increased cholinergic levels were induced by exogenous applications; however, in the awake animal, endogenous activation of the cholinergic system probably provides the required levels of cortical ACh for both memory formation[5,8] and recall[25]. □

Methods

Animal preparation and electrophysiology

Experiments were carried out on adult Wistar albino rats (300±25 g) obtained from the Animal Breeding Unit of The Weizmann Institute of Science. Maintenance, manipulations and surgery were according to institutional animal welfare guidelines. Experimental procedures were similar to those used previously[26,27]. Briefly, anaesthetized rats (urethane, 1.5 g kg^{-1}) were mounted in a modified stereotaxic device[28] which allows free access to the somatosensory cortex and to vibrissae. The right postero-medial barrel subfield was exposed, the dura removed and neural activity recorded with a multi-electrode array composed of two tungsten-in-glass electrodes and a combined electrode[29] composed of a tungsten core surrounded by six micropipettes. The pipettes were filled with acetylcholine chloride (1 M, pH 4.5), atropine sulphate (0.1 M, pH 4.5) and NaCl (3 M) for current balance. In most cases, the tungsten-in-glass and combined electrodes were lowered independently into different barrels. Data from units recorded by the combined electrodes ($n = 132$) and the tungsten-in-glass electrodes ($n = 52$) were analysed separately.

Vibrissae stimulation and protocol

Whiskers were stimulated by a linear electromagnetic vibrator (pulses of 10 ms, 5-ms rise time and 5-ms fall time, 160 μm at ~5 mm from the snout). Temporal frequency tuning curves (TFTCs) were obtained by deflecting the principal vibrissa at different frequencies in the following order: 2, 5, 8, 11 and in a few cases 14 Hz; 45 s interval; (14), 11, 8, 5, 2 Hz, with interblock intervals of 10 s. Stimuli were applied at each frequency in blocks of 12 consecutive trains of 4 s + 1 s intertrain interval each. Before pairing, the TFTC was determined first without and then during ACh iontophoresis. Pairing consisted of 24 trains of stimulation (each of 4 s + 1 s intertrain interval) of the vibrissa at one fixed temporal frequency (5, 8 or 11 Hz) accompanied with ACh iontophoresis (20–80 nA). After pairing, the TFTC was determined without ACh and once again with ACh. In some experiments ($n = 16$ cells), two additional TFTCs were determined, one during combined iontophoresis of ACh and atropine (60 nA) and another during ACh application alone. For 53 cells out of 119 only one pairing was applied. For the other recordings, the pairing was repeated several times at the same or different frequencies.

Data analysis

To keep the initial state comparable among cells, only the first paired frequency was considered for statistical tests. The effect was assessed systematically on the test period immediately after the last pairing at that frequency. The relative strength of the response to a given frequency was quantified by the weighted ratio (WR) = $(R_f - \mathrm{Avg}R) / (R_f + \mathrm{Avg}R)$, where R_f is the response to stimulation at a given frequency (spike count over 60 ms from the stimulus onset) and Avg$R$ is the averaged response to stimulation at all other frequencies. This ratio, which takes values from −1 to +1, was calculated for each of the 24 trains of stimuli, with R_f and Avg$R$ values computed from corresponding trains across frequencies presented during the same TFTC. To assess the effect of conditioning, the 24 values obtained from TFTCs before and after pairing were statistically compared (two-tailed Kolmogorov-Smirnov, significance level $P < 0.01$). The comparison was performed independently for the TFTCs obtained without and with ACh, for each frequency. To assess the frequency specificity of the effect, cells were grouped as a function of the paired frequency (5, 8 or 11 Hz), and the differences in weighted ratios were averaged across cells (see Fig. 3d–f). This analysis was done on all cells showing a statistically significant change in weighted ratio values for any of the tested frequencies (paired and non-paired), thus avoiding any bias towards the paired frequency. The weighted values were statistically compared using multi-factor ANOVA with repeated measures.

Received 8 October; accepted 15 November 1999.

1. Izquierdo, I. in *Neurobiology of Learning and Memory* (eds Lynch, G., McGaugh, J. L. & Weinberger, N. M.) 333–358 (Guilford, New York, 1984).
2. Gordon, W. C. & Klein, R. L. in *Animal Learning and Cognition* (ed. Mackintosh, N. J.) 255–279 (Academic, San Diego, 1994).
3. Mesulam, M. M., Mufson, E. J., Wainer, B. H. & Levey, A. I. Central cholinergic pathways in the rat: an overview based on an alternative nomenclature (Ch1–Ch6). *Neuroscience* **10,** 1185–1201 (1983).
4. Richardson, R. T. & DeLong, M. R. A reappraisal of the functions of the nucleus basalis of Meynert. *Trends Neurosci.* **11,** 264–267 (1988).
5. Singer, W. in *Brain Organization and Memory: Cells, Systems, and Circuits* (eds McGaugh, J. L., Weinberger, N. M. & Lynch, G.) 211–233 (Oxford Univ. Press, New York, 1990).
6. Ahissar, E. & Ahissar, M. Plasticity in auditory cortical circuitry. *Curr. Opin. Neurobiol.* **4,** 580–587 (1994).
7. Weinberger, N. M. Dynamic regulation of receptive fields and maps in the adult sensory cortex. *Annu. Rev. Neurosci.* **18,** 129–158 (1995).
8. Dykes, R. Mechanisms controlling neuronal plasticity in somatosensory cortex. *Can. J. Physiol. Pharmacol.* **75,** 535–545 (1997).
9. Edeline, J. M. Learning-induced physiological plasticity in the thalamo-cortical sensory systems: a critical evaluation of receptive field plasticity, map changes and their potential mechanisms. *Prog. Neurobiol.* **57,** 165–224 (1999).
10. Metherate, R. & Weinberger, N. M. Acetylcholine produces stimulus-specific receptive field alterations in cat auditory cortex. *Brain Res.* **480,** 372–377 (1989).
11. Edeline, J. -M., Hars, B., Maho, C. & Hennevin, E. Transient and prolonged facilitation of tone-evoked responses induced by basal forebrain stimulations in the rat auditory cortex. *Exp. Brain Res.* **97,** 373–386 (1994).
12. Kilgard, M. P. & Merzenich, M. M. Cortical map reorganization enabled by nucleus basalis activity. *Science* **279,** 1714–1718 (1998).
13. Kilgard, M. P. & Merzenich, M. M. Plasticity of temporal information processing in the primary auditory cortex. *Nature Neurosci.* **8,** 727–731 (1998).
14. Rasmusson, D. D. & Dykes, R. W. Long-term enhancement of evoked potentials in cat somatosensory cortex produced by co-activation of the basal forebrain and cutaneous receptors. *Exp. Brain Res.* **70,** 276–286 (1988).
15. Jacobs, S. E. & Juliano, S. L. The impact of basal forebrain lesions on the ability of rats to perform a sensory discrimination task involving barrel cortex. *J. Neurosci.* **15,** 1099–1109 (1995).
16. Baskerville, K. A., Schweitzer, J. B. & Herron, P. Effects of cholinergic depletion on experience-dependent plasticity in the cortex of the rat. *Neurosci.* **80,** 1159–1169 (1997).
17. Maalouf, M., Miasnikov, A. A. & Dykes, R. W. Blockade of cholinergic receptors in rat barrel cortex prevents long-term changes in the evoked potential during sensory preconditioning. *J. Neurophysiol.* **80,** 529–545 (1998).
18. Sachdev, R. N., Lu, S. M., Wiley, R. G. & Ebner, F. F. Role of the basal forebrain cholinergic projection in somatosensory cortical plasticity. *J. Neurophysiol.* **79,** 3216–3228 (1998).
19. Woolsey, T. A. & Van der Loos, H. The structural organization of layer IV in the somatosensory region (SI) of mouse cerebral cortex. The description of a cortical field composed of discrete cyto-architectonic units. *Brain Res.* **17,** 205–242 (1970).
20. Carvel, G. E. & Simons, D. J. Biometric analyses of vibrissal tactile discrimination in the rat. *J. Neurosci.* **10,** 2638–2648 (1990).
21. Ahissar, E., Haidarliu, S. & Zacksenhouse, M. Decoding temporally encoded sensory input by cortical oscillations and thalamic phase comparators. *Proc. Natl Acad. Sci. USA* **94,** 11633–11638 (1997).
22. Webster, H. H. *et al.* Long-term enhancement of evoked potentials in racoon somatosensory cortex following co-activation of the nucleus basalis of Meynert complex and cutaneous receptors. *Brain Res.* **545,** 292–296 (1991).
23. Howard, M. A. & Simons, D. J. Physiologic effects of nucleus basalis magnocellularis stimulation on rat barrel cortex neurons. *Exp. Brain Res.* **102,** 21–33 (1994).
24. Ahissar, E., Haidarliu, S. & Shulz, D. E. Possible involvement of neuromodulatory systems in cortical Hebbian-like plasticity. *J. Physiol. (Paris)* **90,** 353–360 (1996).
25. Delacour, J., Houcine, O. & Costa, J. C. Evidence for a cholinergic mechanism of "learned" changes in the responses of barrel field neurons of the awake and undrugged rat. *Neuroscience* **34,** 1–8 (1990).
26. Shulz, D. E., Cohen, S., Haidarliu, S. & Ahissar, E. Differential effects of acetylcholine on neuronal activity and interactions in the auditory cortex of the guinea-pig. *Eur. J. Neurosci.* **9,** 396–409 (1997).
27. Haidarliu, S. & Ahissar, E. Spatial organization of facial vibrissae and cortical barrels in the guinea pig and golden hamster. *J. Comp. Neurol.* **385,** 515–527 (1997).
28. Haidarliu, S. An anatomically adapted, injury-free headholder for guinea pigs. *Physiol. Behav.* **60,** 111–114 (1996).
29. Haidarliu, S., Shulz, D. E. & Ahissar, E. A multi-electrode array for combined microiontophoresis and multiple single-unit recordings. *J. Neurosci. Meth.* **56,** 125–131 (1995).

Supplementary information is available on *Nature*'s World-Wide Web site (http://www.nature.com) or as paper copy from the London editorial office of *Nature*.

Acknowledgements

We thank Y. Dudai, Y. Frégnac, H. Markram, P. Salin and M. Segal for helpful comments, and A. Bagady for help with statistical analysis. V.E. and D.E.S. were supported by the

French Embassy in Israel during their visits to the laboratory of E.A. where the experiments were done. This work was supported by PICS CNRS, Ministère des Affaires Etrangères Français, AFIRST, HFSP, US-Israel Binational Science Foundation, Israel and the MINERVA Foundation, Germany.

Correspondence and requests for materials should be addressed to D.E.S. (e-mail: shulz@iaf.cnrs-gif.fr).

Modulation of A-type potassium channels by a family of calcium sensors

W. Frank An*, Mark R. Bowlby†, Maria Betty†, Jie Cao*, Huai-Ping Ling†, Grace Mendoza†, Joseph W. Hinson†, Karen I. Mattsson†, Brian W. Strassle†, James S. Trimmer‡ & Kenneth J. Rhodes†

**Millennium Pharmaceuticals, Cambridge, Massachusetts 02139, USA*
† *Neuroscience Division, Wyeth-Ayerst Research, Princeton, New Jersey 08543, USA*
‡ *Department of Biochemistry and Cell Biology, SUNY, Stony Brook, New York 11794, USA*

In the brain and heart, rapidly inactivating (A-type) voltage-gated potassium (Kv) currents operate at subthreshold membrane potentials to control the excitability of neurons and cardiac myocytes[1,2]. Although pore-forming α-subunits of the Kv4, or *Shal*-related, channel family form A-type currents in heterologous cells[3], these differ significantly from native A-type currents. Here we describe three Kv channel-interacting proteins (KChIPs) that bind to the cytoplasmic amino termini of Kv4 α-subunits. We find that expression of KChIP and Kv4 together reconstitutes several features of native A-type currents by modulating the density, inactivation kinetics and rate of recovery from inactivation of Kv4 channels in heterologous cells. All three KChIPs co-localize and co-immunoprecipitate with brain Kv4 α-subunits, and are thus integral components of native Kv4 channel complexes. The KChIPs have four EF-hand-like domains and bind calcium ions. As the activity and density of neuronal A-type currents tightly control responses to excitatory synaptic inputs, these KChIPs may regulate A-type currents, and hence neuronal excitability, in response to changes in intracellular calcium.

A-type Kv currents formed by Kv4-family α-subunits control excitatory responses in neuronal cell bodies and dendrites[1,3–7] and contribute to repolarization following action potentials in cardiac myocytes[2]. Here we used the yeast two-hybrid (YTH) system[8] to identify proteins that modulate Kv4 channels. We constructed a YTH bait corresponding to the intracellular amino terminus (amino acids 1–180) of the rat Kv4.3 subunit and screened an oligo dT-primed library of rat midbrain complementary DNA to identify proteins that interacted with it. Many proteins that strongly interacted with the Kv4.3 N-terminal bait also interacted with the N-terminal 180 amino acids of Kv4.2, but not with Kv1.1 or other, unrelated baits (Fig. 1a). Among the Kv4-specific interactors were two new members of a previously described gene family (see below), here termed KChIP1 and KChIP2. Library screening and database mining identified mouse and human orthologues of these genes, as well as expressed sequence tags (ESTs) encoding a previously identified member of this family (KChIP3). Northern blot analysis of rat (KChIP1 and KChIP2) or mouse (KChIP3) tissues revealed that KChIP1 is predominantly expressed in brain, KChIP2 is expressed in heart, brain and lung, and KChIP3 is highly expressed in brain with lower expression in testes (Fig. 1b).

The KChIP1, 2 and 3 cDNAs encode 216-, 252- and 256-amino-acid polypeptides, respectively, which have distinct N termini but share ~70% amino-acid identity throughout a carboxy-terminal 185-amino-acid 'core' domain containing four EF-hand-like motifs (Fig. 2). Although these KChIPs have around 40% amino-acid similarity to neuronal calcium sensor-1 (NCS-1) and are members of the recoverin/NCS subfamily of calcium-binding proteins[9] (Fig. 2), other members of this subfamily (such as hippocalcin) did not

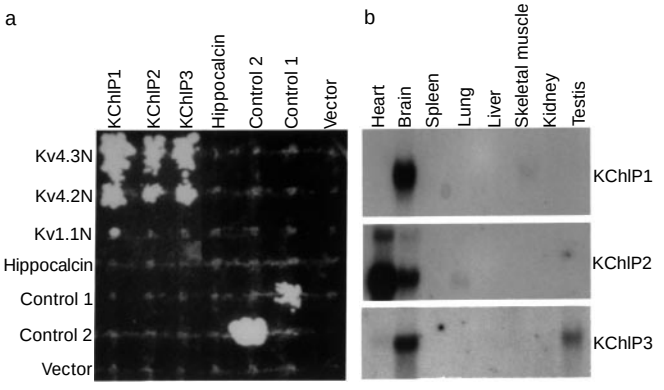

Figure 1 YTH interaction and tissue expression of KChIPs1–3. **a**, Growth on the seventh day on a Trp-Leu-His synthetic dropout plate (with 10 mM 3-AT) demonstrating the specific interaction of KChIPs1-3 with Kv4 α-subunits. KChIP1, KChIP2, KChIP3 and hippocalcin are in the 'fish' configuration (columns); N-terminal domains of Kv4.3, Kv4.2, Kv1.1 and hippocalcin are in the 'bait' configuration (rows). Control 1 and control 2 are two interacting fish/bait pairs, respectively, unrelated to K^+ channels or the KChIPs. **b**, Northern blots (Clontech) showing the expression of KChIP mRNAs across rat (KChIP1 and KChIP2) and mouse (KChIP3) tissues.

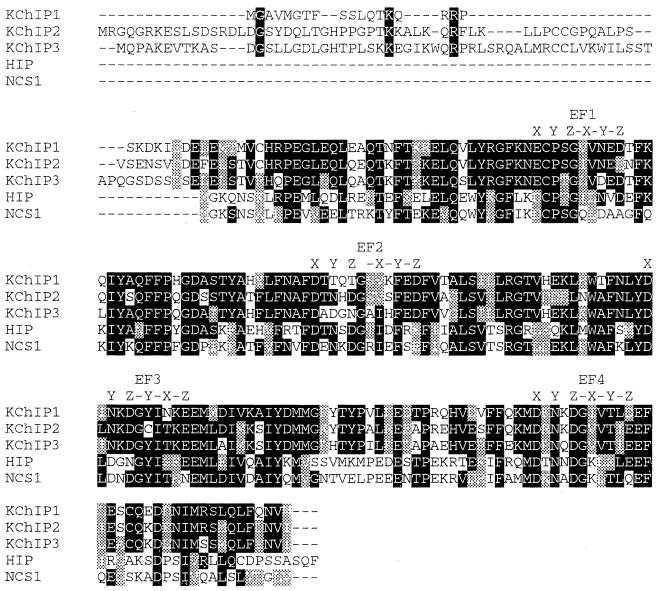

Figure 2 Sequence alignment of human KChIPs with members of the recoverin family of Ca^{2+}-sensing proteins. The alignment was performed using CLUSTALW[21]. Residues identical to the consensus are shaded black and conservative substitutions are shaded grey. X marks position 1 of the 12-amino-acid consensus EF-hand motif, as defined in PROSITE[22]. X, Y, Z and -X, -Y, -Z denote EF-hand Ca^{2+}-binding residues. Like all members of the recoverin family, the KChIP EF1 diverges significantly from the EF-hand consensus and contains a Cys-Pro motif. HIP, human hippocalcin; NCS1, rat neuronal calcium sensor-1.